CLASSIFICATION OF EYELID POSITION AND EYEBALL MOVEMENT USING EEG SIGNALS

R. Ramli[1], H. Arof[2], F. Ibrahim[3], M. Y. I. Idris[4], A.S.M. Khairuddin[5]

[1,3]Department of Biomedical Engineering, Faculty of Engineering, University of Malaya, 50603, Kuala Lumpur, Malaysia.
[1,2,3]Centre for Innovation in Medical Engineering, Faculty of Engineering, University of Malaya, 50603, Kuala Lumpur, Malaysia.
[2,5]Department of Electrical Engineering, Faculty of Engineering, University of Malaya, 50603, Kuala Lumpur, Malaysia.
[4]Department of Computer System and Technology, Faculty of Computer Science & Information Technology, University of Malaya, 50603 Kuala Lumpur, Malaysia.

Email: roziana.ramli@gmail.com[1], ahamzah@um.edu.my[2], fatimah@um.edu.my[3], yamani@um.edu.my[4], anissalwa@um.edu.my[5]

ABSTRACT

Contamination of EOG activities in EEG signals remains a significant problem in designing the hybrid BCI system. Since EEG signals have always been contaminated by EOG artifacts, we employ these artifacts as inputs into our system. Therefore, in this study we utilized theEEG and its EOG artifacts as inputs to the hybrid BCI and evaluated the classification performance between thresholding and classifier techniques to determine the eyelid position and eyeball movement from EEG signals and its EOG artifacts in real-time. The EEG signals are recorded from the occipital (channel O2) and motor cortex (channel C3 and C4) on the scalp using 10-20 montage system. First, alpha band signal at channel O2 is monitored and analyzed to determine the eyelid position of eye closed and open. If the eyes are open, EOG traces in two delta band signals related to horizontal eyeball movement at channel C3 and C4 are examined to obtain the eyeball movement classification. A sliding window frame is utilized to analyze the EOG trace signals so that important cues are positioned at the center of the window for effective classification. A few features can be extracted from the EEG data in the window and utilized to determine the eyelid position and eyeball movement by thresholding. The data can also be utilized directly as inputs to MLP or SVM classifiers and their performances are compared with the thresholding scheme. The highest classification rate of 0.98% is obtained by the SVM classifiers with an average execution time of just 0.53s. The result of this classification can be utilized in hybrid BCI for various applications.

Keywords: EEG signals, EOG artifacts, Hybrid BCI, Eyeball Movement, Eyelid Position, Real-time.

1.0 INTRODUCTION

The variety of Human Machine Interface (HMI) for assistive applications has been proposed in many studies to help those with disabilities [1-3]. Alternative strategies using bio-signal (i.e., electroencephalography (EEG), electrooculography (EOG) and electromyography (EMG))demand lesser control of the body functions for controlling HMI[4].These strategies are suitable for those with severe motor disabilities or suffered from locked-in syndrome.However, each approach has its own advantages and disadvantages. For instance, EMG signals can be measured from various types of muscle in any part of the body. On the other hand, EEG and EOG signals can only be measured from the scalp and outer canthi respectively. Unlike EEG, EMG and EOG signals has higher amplitude and signal-to-noise ratio (SNR). EEGis difficult to modulate and always contaminated with noise from other bio-signals. In the cases of extreme motor impairment condition, it is expected that number of muscles can be explored are limited while cognitive activity and eye movements are mostly preserved[5]. These limitations have led researchers to develop a hybrid HMI that combines different approaches to utilize the advantages of multiple bio-signals in a system. The use of hybrid HMI will reduce the errors as well as increase the robustness of the interface.

EEG based HMI is also known as Brain Computer Interface (BCI), which can translate the user's intention into computer commands.This user's intention will generate a unique EEG pattern, which can be evoked by external stimuli and known as event related potential (ERP).An ERP can be analyzed in five main frequencybands, Delta (θ), Theta (θ), Alpha (α), Beta (β) and Gamma (γ) and these frequency bands can be defined according to distribution over the scalp or biological significance[6]. Various components of ERP (e.g, P300 response, mu and beta rhythms, motor imagery and steady-state visual evoked potentials (SSVEP))has been introduced as input of BCI to control external devices (e.g., character selection [7-9], virtual object movement [10], image selection [11], cursor movement [12-15] and wheelchair navigation [16-20]) to assist physically challenged patients.

The combination ofEEG with additional signal from EEG or other physiological sources such as EOG or EMG for real world applications are known as hybrid BCI[21].This strategy can improve the BCI performance, as the false positive from two sources would be needed for a misclassification to occur. The hybrid BCI is typically processed simultaneouslyor operating two systems sequentially with the first system can act as either a "brain switch" or as "selector"[22].It isdemonstrated that the combination of various ERP components could improve the classification accuracy of BCI[23]. In recent years, hybrid BCI is proposed to produce multiple control commands for applications.For instance, the P300 potential and motor imagery or SSVEP areincorporated to control the 2-D cursor and brain-actuated wheelchair[24, 25]. These systems provide multiple commands for multi-dimensional control such as controlling direction and speed.Simultaneously, hybrid BCI combined motor imagery and SSVEP signals havebeen established for control engineering [26, 27]. In this approach, the control commands are limited by a small number of classification categories. Moreover, Pfurtscheller et al. designed a motor imagery based brain switch for activating and deactivating their hybrid BCI system [28]. These hybrid BCIs achieve better control effect for external device control, but it still a challenge to design a hybrid BCI system for high-efficiency control.

Generating P300, mu and beta rhythms,Steady State Visually Evoked Potential (SSVEP) and motor imagery signalsrequire a high degree of concentration and cancause difficulties to attain effective control ofhybrid BCI[29].In opposite, acquiring EOG signal is trivial and no special training is required to execute voluntary eye movement. For severely paralyzed patients, signals (e.g., EOG) tends to be stable with the exception of cerebral palsy [30]and multiple sclerosis [31].Therefore, a combination with other bio-signal (e.g., EEG) can provide a more efficient channel for interaction.For instance, Postelnicu et al. demonstrates that controlling a robotic arm is more easier and accurate using a combination of EEG and EOG rather than EOG alone [32]. Moreover, the implementation of this hybrid BCI can improve the response time when a selected command is given[33].This feature is important when astop command is sent to abrain controlled wheelchair, andthe wheelchair stopsas fast as possible after the command is received to avoid any collisions[34].Fatigue is unavoidablein a long-term use of hybrid BCI, thus Usakli et al. proposed a system to switches between P300 and EOG without learning a new user interface [35]. In hybrid BCI system, the contamination of ocular artifact remains a significant problem, specifically for the system that relies on eye movements as input.Since the EEG signals have always been contaminated by EOG artifacts,we employ these artifacts as a secondary input to our asynchronoushybrid BCI system.

EOG artifacts in EEG signals generate high amplitude signals(i.e., larger in the frontal area and decrease rapidly towards the posterior area)[36]. In this study, we develop a hybrid BCIsystem that utilizes a combination of EEG alpha signal (8-13Hz) and EOG artifacts in delta band (<3Hz) as inputs to determine the user's eyelid position and eyeball movement respectively. The alpha band signal is recorded from the occipital region while the delta band signals are obtained from the motor cortex. Features (e.g., variance and central tendency measurement (CTM))can be extracted from the EEG data in the window and utilizedto determine the eyelid position and eyeball movement by using thresholding. The data can also be utilized directly as inputs to a classifier (e.g., multilayer perceptron(MLP) or support vector machine(SVM)). MLP and SVM are common classifiers that have been utilized by many researchers to classify EEG or EOG signals[37, 38]. In the experiment, the classification performances of the thresholding, MLP and SVM classifiers are compared and presented in tables.

The paper is organized as follows. First, methodology of this work is presented. Then, signal processing and classification techniques employed in this work are elaborated. Subsequently, performed experiment results are discussed. Finally, conclusions and future works are outlined.

2.0 METHODS

The EEG data areacquired using g.Mobilab from Guger Technologies at a sampling rate of 256Hz. The gold electrodes are placed at C3, C4and O2 with reference connected to Cz and ground attached at forehead (FPz). The electrode arrangement followsthe International 10-20 montage system and the impedance ismaintained below 10kΩ. Since the experiment isconducted in unshielded room, the laptop and g.MOBIlabarepowered by battery to minimize electrical interference contamination in the EEG data. The EEG signals areacquired and analyzed using LabVIEW software from National Instrument.

There are 20 healthy participants involved in this study, with age ranging between 23 to 27 years old. All participants arefree from any neurological disease and hasno prior experience with EEG recording. Theyarebriefed on the purpose and nature of the study and asked to sign a consent form before the EEG recording begin. The experimental procedure complies with the Declaration of Helsinski.

2.1 Experimental procedure

The study isconducted in two separate sessions,training and testing sessions. In the training session, EEG signalsarerecordedand analyzed to determine threshold values needed for sliding window,CTM and variance. The data are also utlizedfor training the MLP and SVM classifiers. Every participantperformes5trials for each instruction of horizontal eyeball movements (from center to left or right and the reverse) and eyelid position (open and closed). A total of 400 trials arerecorded for the horizontal eyeball movements and 200 trials for eyelid position from 20 participants. Each trial isrecorded in 10 secondsand15 seconds rest in between eyeball movements and eyelid position trials.

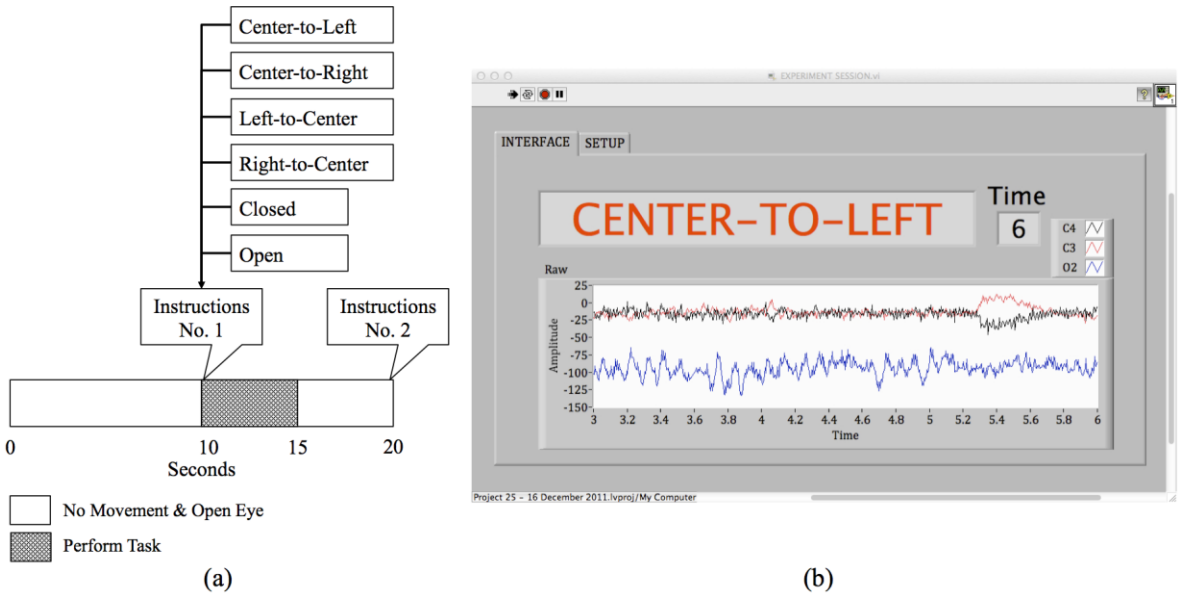

Fig.1:(a) 6instructions of horizontal eyeball movements and eyelid position areassigned every 10 seconds in the testing session. The subject must respond accordingly within 5 seconds and no restriction of eye blinking during the experimental session. (b) Graphical user interface during the experimental session.

The testing session is conducted to test the efficiency of signal processing by usingthresholding and classifiers in real-time. Fig. 1(a) shows aninstruction is assigned in every 10 seconds. The subject is given 5 seconds to respond correctlyfor each instruction. In total, participants perform 400 trials for horizontal eyeball movements and 200 trials for eyelid positions. The performance of each participant is recorded and analyzed.

2.2 Signal properties

The filtered alpha signal in channel O2 shows a higher event related potential (ERP) fluctuation during eye closingcomparedto eye opening. The peak of the alpha signal is 5-10uV during eye openingand 20-50μV when eyesare closedas shown in Fig.2. However, the amplitude of the signal itself varies with individuals. The natural blink and eyeball movement that occur during eye opening are negligible in the alpha band at the occipital region [39]. Conversely, natural blink and vertical eyeball movement generate artifacts in delta band.These artifacts are larger in the frontal and decrease rapidly towards the posterior areas [36].

In this study, the horizontal eyeball movement is actually inferred from the delta signal in channel C3 and C4 due to the minimal presence of blink and vertical eyeball movement. When the eyeball moves from the center to the right, a short positive pulse is observed in channel C4. At the same time, a weak negative pulse is noticeable in channel C3. Then, when the eyeball shifts from right to center, a long positive pulse is observedat channel C3 and negative pulse at channel C4.The reverse characteristics can be observed during eyeball movement from the center to left and return to center.These signals are utilizedas inputs to a classifier to track changes in eyeball movement.

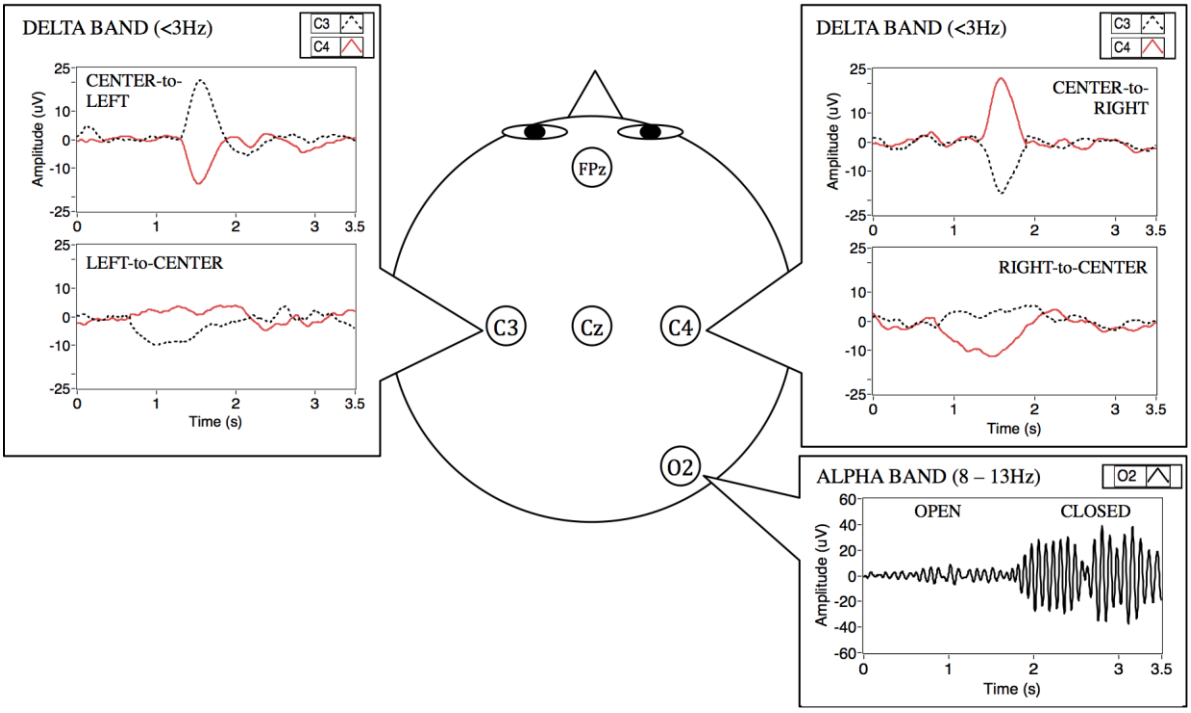

Fig.2: The EEG signals areacquired at channel C3, C4, O2 with Cz as reference. In delta band (<3Hz), a short positive pulse is observed at channel C4 and negative pulse at channel C3 when the eyeball direction is moving from center to right. When the eyeball shifts from right to center, a longer positive pulse can be observed at channel C3 and negative pulse at channel C4. The reverse characteristics can be observed during eyeball movement from the center to left and return to center. In alpha band (8-13Hz) at channel O2, the closed eye exhibits more alpha signal activity in the occipital region.

3.0 SIGNAL PROCESSING AND ANALYSIS

The signal processing schemefor the classification of eyelid position and horizontal eyeball movements is summarized in Fig.3. First, the O2 signal is processed by using Butterworth bandpass filter to capture alpha signal within 8-13Hz.Simultaneously, signal inchannel C3 and C4 are processed by usingButterworth lowpass filter to capture delta signal(i.e., remove all signal content in >=3Hz). Then, these signals are analyzed in a window of 128 samples for every 0.5 second, making two consecutive windows non-overlapping in 1second.

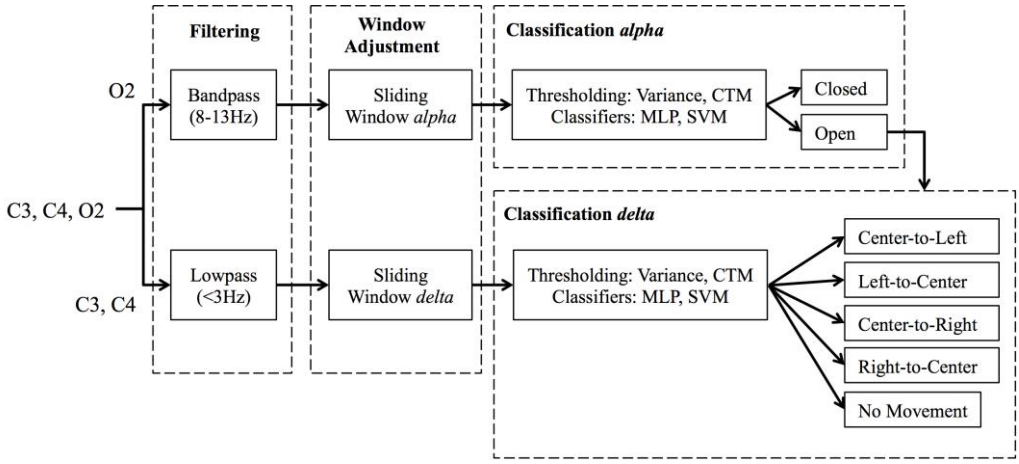

Fig.3: Signal processing scheme for identification of eyelid position in alpha band (8-13Hz) at O2 and horizontal eyeball movements in delta band (<3Hz) at C3, C4.Performances of the classification are compared between classifiers and thresholding scheme.

3.1 Sliding window

When monitoring the alpha signal inchannel O2, a conventional window frame capturesthe signal amplitude in transition from low to high when the open eyes are just about to closeand vice versa.Consequently, samples in the window are the mixture of closed and open eyes as showed inFig.4(b).Therefore, a non-rigid sliding window is utilizedto shift the position of thewindow so that it onlycontain samples of closed or open eyes exclusively. For O2 signal, the sliding window is adjusted as follows

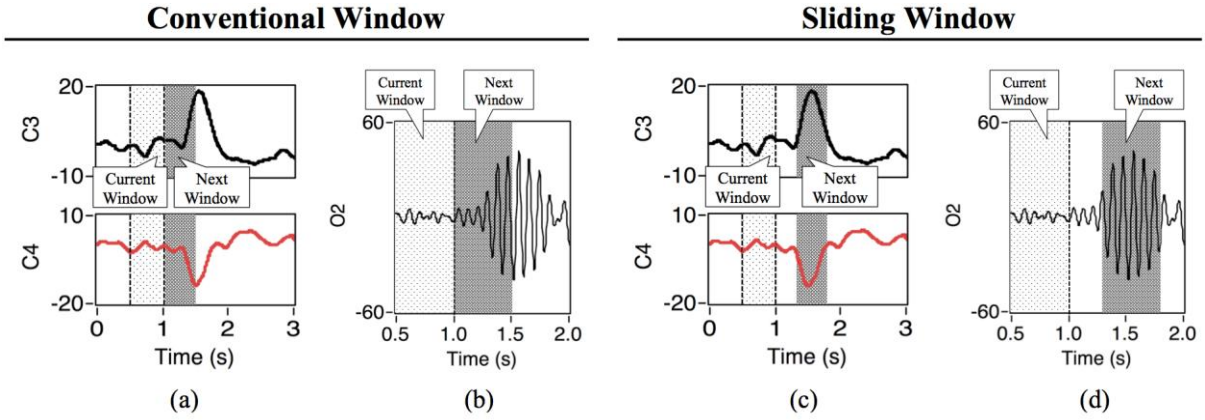

Fig.4: (a), (b) The conventional window will lose part of the crucial features in the signal. Insufficient information in a window will lead to misclassification. (c), (d) Sliding window will automatically adjust its position so that the full cue is captured within its interval.

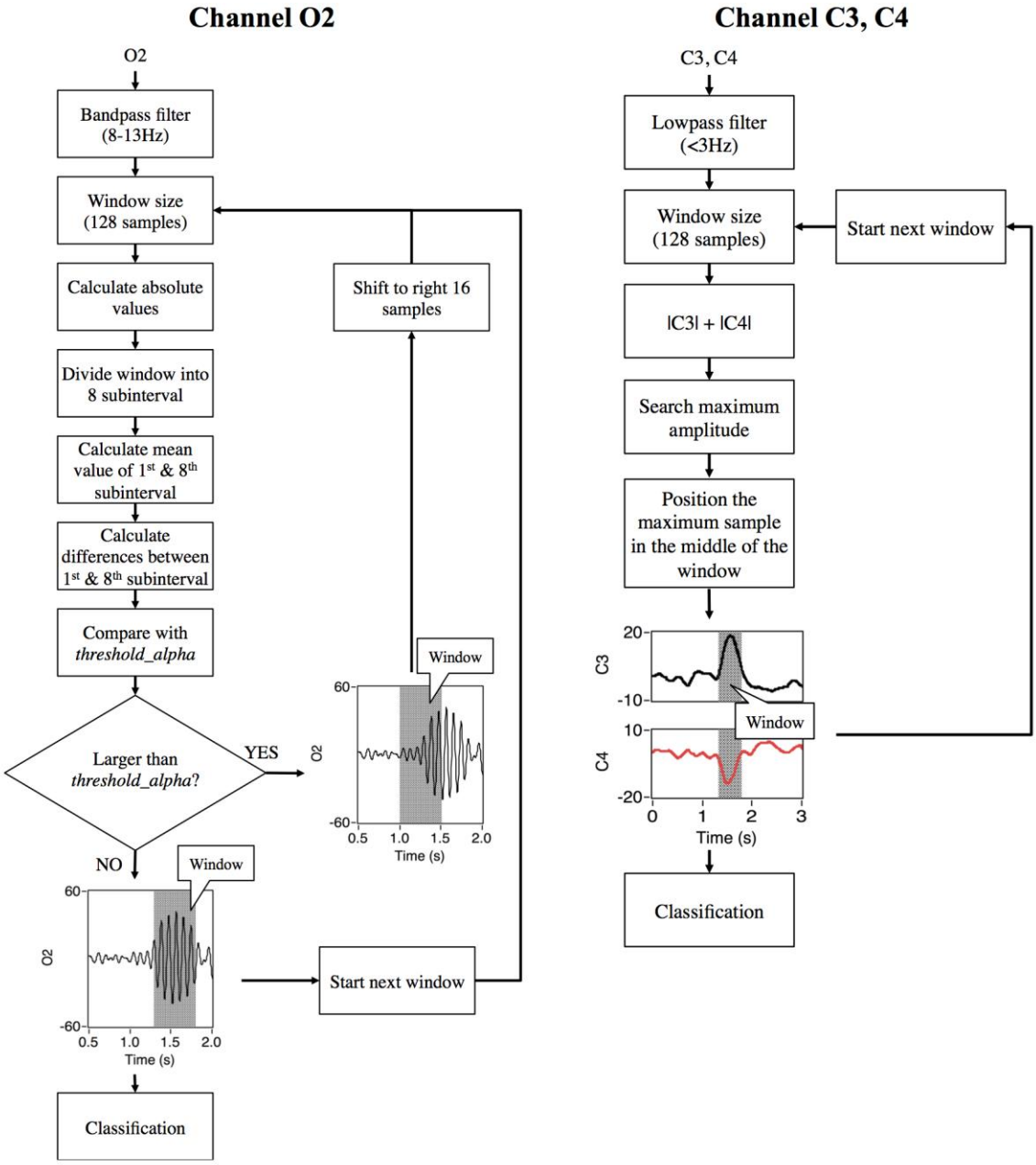

Fig.5: The process to shift position of sliding window. The *threshold_alpha* is set at half of the average of the absolute values in a window during closed eye. If O2 window is adjusted, the C3 and C4 window will follow its position. Otherwise, the O2 window will follow the position of the C3 or C4 window.

Initially, the absolute values of 128 samples in a window are calculated. Then, these values are divided into eightnon-overlapping subintervals containing 16 samples. Next, the sum of the absolute values of data are calculated and averaged in the first and last subintervals. The window is shifted to the right by 16 samples if the difference between first and last subintervalsexceeds a threshold (called *threshold_alpha*)and repeated the shifting step until the difference is less than the *threshold_alpha*. Once the window stop shifting, the samples (data) will be utilized to classify eyelid position. The *threshold_alpha* is set at half of the average of the absolute values in a window during closed eye, as shown in Eq. (1). *Threshold_alpha*is utilized particularly to reposition

the window in channel O2. The total sample of 128 in a window is denoted by N while the x_i represents the discrete data at *i*-th sample in a window.

$$threshold\_alpha = \left(\frac{1}{N}\sum_{i=1}^{N}|x_i|\right)\Big/2 \quad (1)$$

For C3 and C4 signals, the window position is shifted so that the data with the maximum amplitude will be at the center of the window.The absolute value of the C3 sample is added to the absolute value of C4 samplefor each position in the window. Then, the sample with the maximum sum is identified and positioned at the center of the window. The procedure to adjust the window position is illustrated in Fig.5. When O2 window is adjusted, the C3 and C4 window will follow its position. Otherwise, the O2 window will follow the position of the C3 or C4 window. In short, adjustment to the position of the O2 window takes precedence over that of the C3 and C4 window.

3.2 Eyelid position and eyeball movement analysis

In classification, the alpha signal from O2 is analyzed to ascertain the eyelid position of open and closed eyes. If the eyes are open, the eyeball direction is determined from the delta band in C3 and C4. Variance and CTM features are extracted from EEG data and utilizedas input forthresholding, while MLP and SVM classifiers will directly utilizedthe filtered EEG data. These techniques areselected based on their low computational complexity and performance reported in the previous studies [40, 41]. All the threshold values and classifiers are determined and trained uniquely with individual's recorded EEG data.

3.2.1 Variance

Variance (σ^2) is a variability measurement of data set from mean andexpected value. The variance of unknown distribution can be computed as in (2)by taking account of mean (μ), number of sample (N) and value of each sample ($x(t)$).

$$\sigma^2 = \frac{1}{N}\sum_{k=0}^{N-1}(x(t)-\mu)^2 \quad (2)$$

The variance is highwhen the differences between samples are more spreaded out [42]. In eyelid position analysis, a threshold (i.e., *variance_closed)*isset at half of thevariance average for closed eyessignals in channel O2 as described in (3). The variance average of closed eyes signals is computed from five closed eyes trials (Tr) recorded for each participant during the training session. For each trial, the variance at sample *k*-th (σ_k^2)is average over the total samples in a trial (N). The alpha signal from a particular window in channel O2 is classified as open eyes if the calculated variance isequal or smaller than the *variance_closed. Whereas,* larger variance is classified as closed eye.

$$variance\_closed = \left(\frac{1}{Tr}\sum_{i=1}^{Tr}\sum_{k=0}^{N-1}\frac{\sigma_k^2}{N}\right)\Big/2 \quad (3)$$

In the eyeball movement analysis, eyeball directions are determined from four thresholds, *variance_rightcenter*, *variance_left*, *variance_leftcenter* and *variance_right* as shown in Fig.6. These thresholds are computed from the mean variance of the eyeball movement over trials from the recorded data using the same principle as in (3). The values for *variance_rightcenter* and *variance_left*are calculated from the delta signals in C3 while *variance_leftcenter* and *variance_right*are calculated from the delta signals in C4. When the open eye is detected, *variance_rightcenter* and *variance_leftcenter* identifies whether the eyeballs are at stationary or moving mode. If the eyeballs are moved, the gaze direction will be determined from *variance_left*

or*variance_right*.In the case of exceeding these thresholds, center-to-left or right movement is detected.Otherwise, return to center movement is detected.

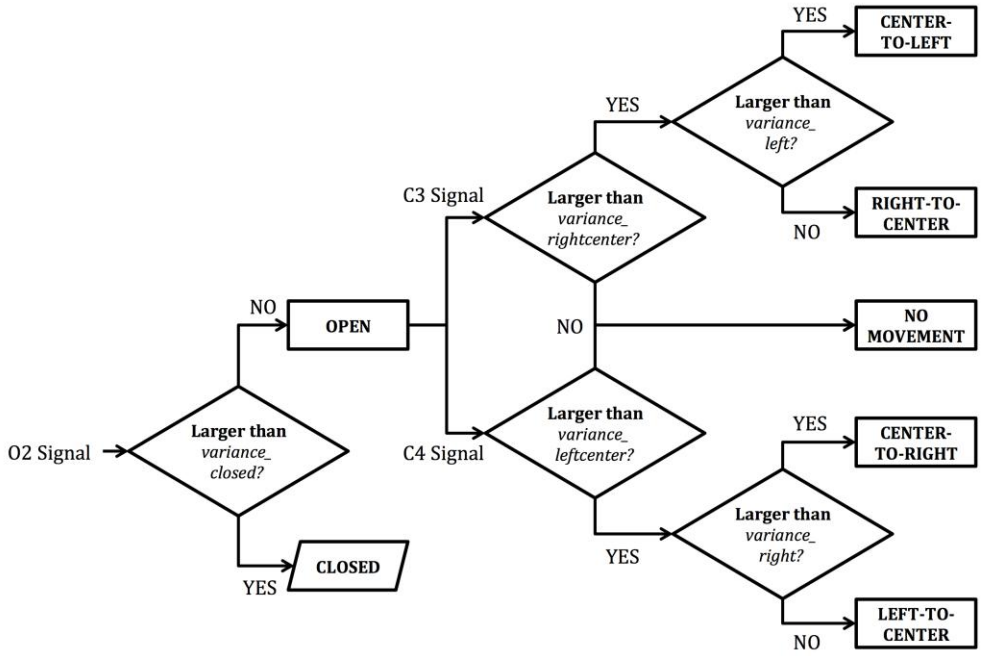

Fig.6: Five threshold values are utilized to determine the eyelid position and eyeball movements. Analysis for C3 and C4 are done simultaneously.

3.2.2 Central tendency measurement (CTM)

Second-order difference plot displays the successive rates of variability against each other where $[x(n+1)-x(n)]$ is plotted against $[x(n+2)-x(n+1)]$. The scaling factors of second-order difference plot increase as the sampling frequency increase. Therefore, higher frequency components have wider data spreading on x, y plane compared to lower frequency components. The CTM measures the variability in the second-order difference plot by counting the points (x) within the radius (r) and dividing by the total numbers of points (n) as describe below in (4) and (5):

$$\mathrm{CTM} = \frac{\sum_{i=1}^{n-2} \delta(d_i)}{n-2} \tag{4}$$

$$\delta(d_i) = \begin{cases} 1 \ if \ \left([x(i+2)-x(i+1)^2] + [x(i+1)-x(i)]^2\right)^{0.5} < r \\ 0 \ otherwise \end{cases} \tag{5}$$

where, $i =$ samples

The CTM value represents the fraction of the total points lie within the radius without distinguishes between sign. The optimum radius ischosen when CTM reaches a value of 0.90 to avoid spurious high frequency noisy components at highradius value [40], i.e., the transient signal due to the filtering performed to extract the alpha band signal as depicted in Fig.7.Then, the radius difference,r_d can be defined in (6) for eyelid position analysis:

$$r_d = r(0.90, eye\_O2) - r_{mean}\ (0.90\ open) \tag{6}$$

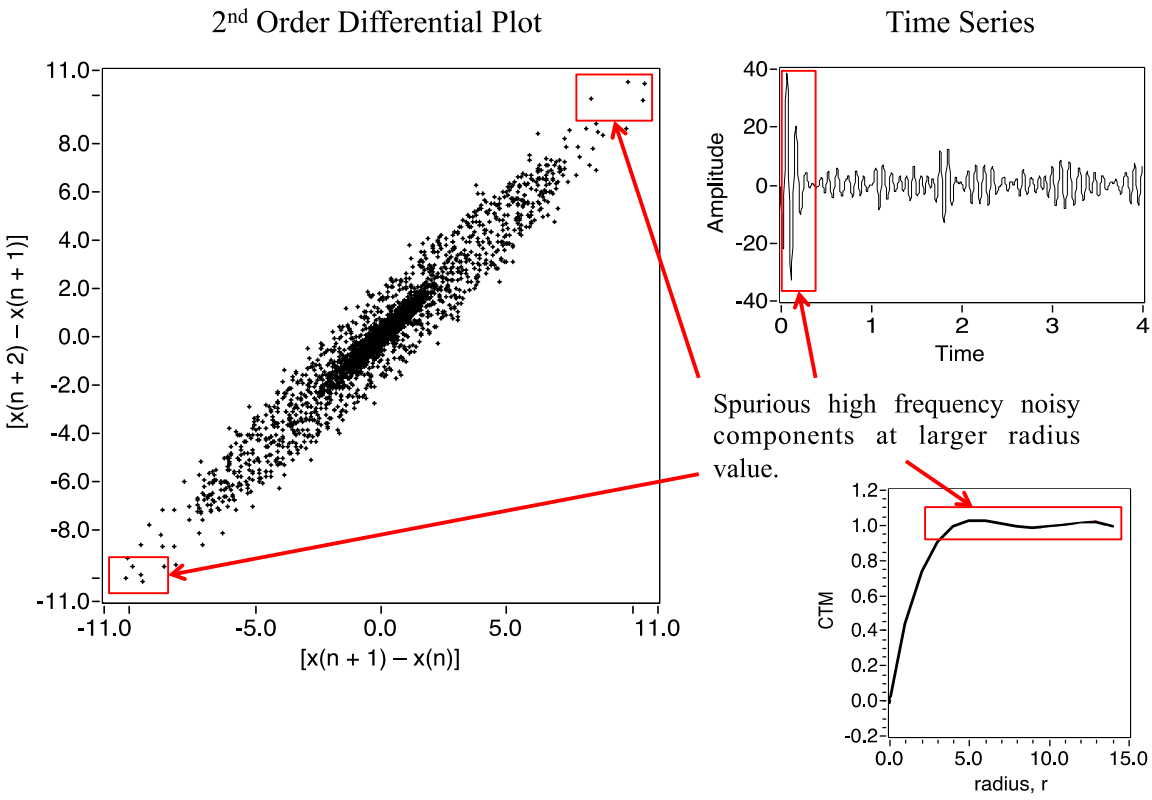

Fig.7: The transient signal due to the filtering performed to extract the alpha band signal causesthe noisy components at larger radius value in 2nd order differential plot.

The mean value of open eyes radius, r_{mean} $(0.90\ open)$iscalculated over collected data. The classification of open and closed eyesisbased on the sign of r_d value from (4). The alpha rhythm of the closed eyes contains higher variability compared to open eyes, thus, the positive value of r_d yields closed eyes condition while negative value yields open eyes condition.

If the open eyes is detected, the proses to determine gaze direction will continue by analyzing delta signal in C3 and C4. First, the radius difference between signals in C3 and C4 is calculated as defined in (7).

$$r_d = r(0.90, eye\_C3) - r(0.90, eye\_C4) \tag{7}$$

If the value of r_d is positive, the signal in C3 is utilized to determine eyeball movement as no movement, center-to-left and right-to-center. Otherwise, signal in C4 isutilized in the analysis. The values of r_{mean} $(0.90\ rightcenter)$, r_{mean} $(0.90\ leftcenter)$, r_{mean} $(0.90\ left)$, r_{mean} $(0.90\ right)$ are computed over radius of eyeball movements from the recorded data. These thresholds are compared with the calculated radius of unknown eyeball movements for classification as illustrated in Fig.8.

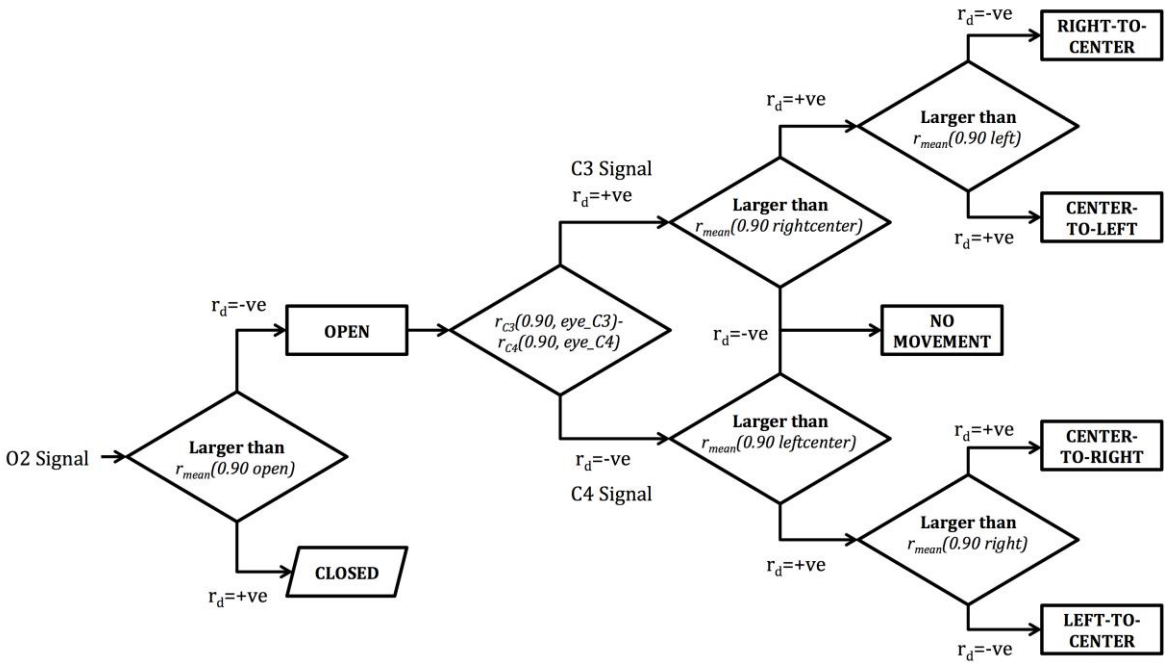

Fig.8: Three mean radiuses when CTM reaches a value of 0.90 areutilized to determine the eyelid position and eyeball movements.

3.2.3 Support vector machine (SVM)

An SVM is a supervised binary classifier that utilizesa decision function to split the data into two classes. Graphically, the decision function can be visualized as a hyperplane separating the classes. In our experiments, Fig. 9 shows five SVM classifiers are utilizedto classify the eyelid position and eyeball direction changes and for all SVMs, quadratic function is utilizedas the kernel. The gamma parameter for the SVM is set at the default value, which is the reciprocal of the number of inputs (in this case it is 1/128).As a supervised classifier, an SVM requires training and signals from the recording session areutilizedto train the SVMs. A total of five SVMs areutilizedto classify eyelid position and eyeball movement. The first SVM decides open eyes and closed conditions using the O2 data. Then, the second SVM takes the C3 and C4 data as inputs to identify whether the eyeballs move or remain stationary. If the eyeballs move, the third SVM classifies the gaze direction movement into two classes (i.e., center to corner or corner to center). The fourth SVM divides the center to corner class into center-to-left and center-to-right classes. Finally, the fifth SVM splits the corner to center class into right-to-center and left-to-center classes.

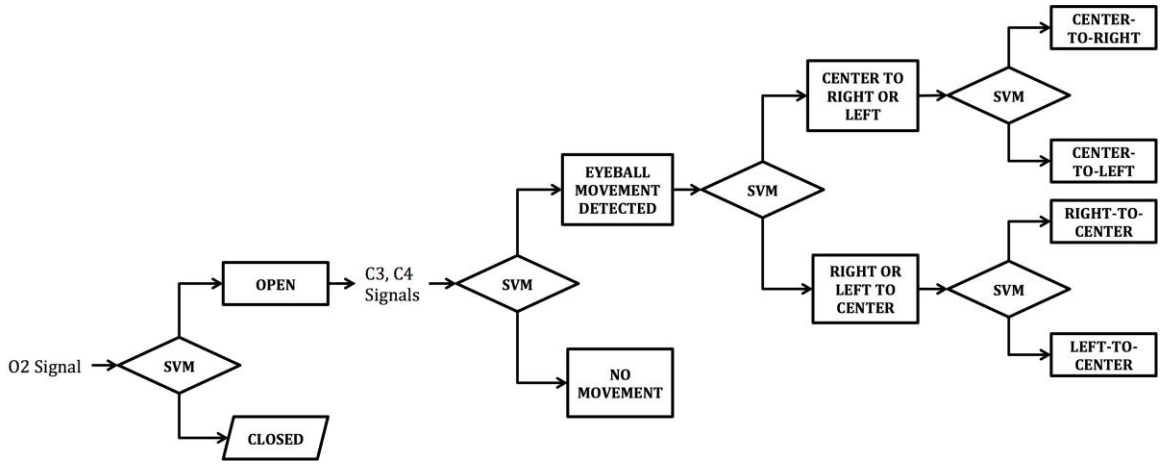

Fig.9: The classification steps to classify the eyelid position and the eyeball movements in SVM.

3.2.4 Multilayer perceptron (MLP)

MLP is a feedforward artificial neural network model. It creates a model tomap the input to the output based on the historical data. Fig.10 illustrates a perceptron network with an implemented hidden layer in this study.

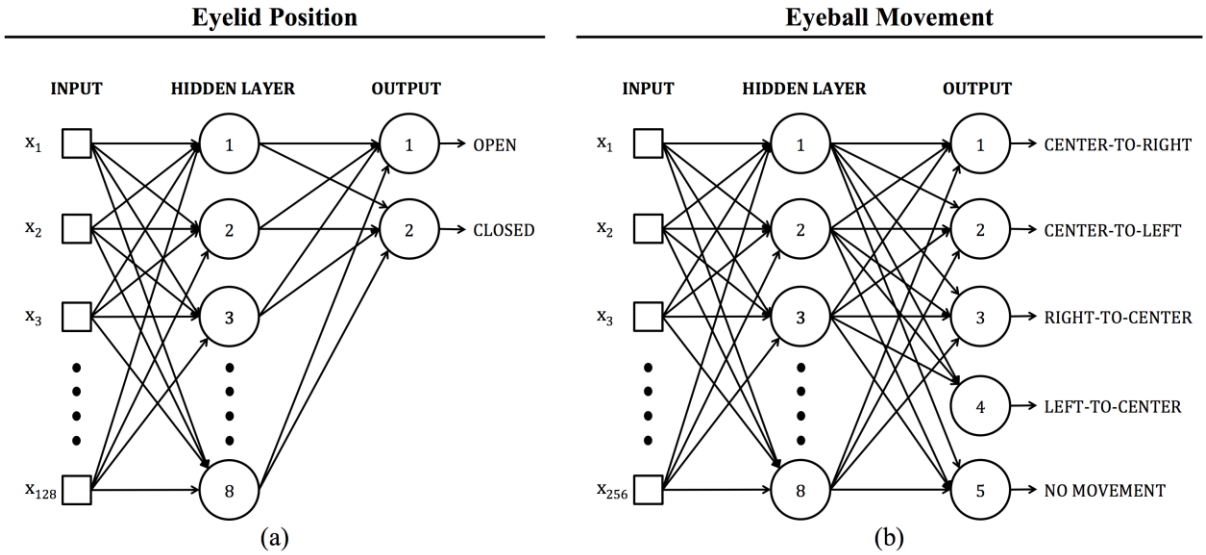

Fig.10: (a) The input layer consists of 128 neurons from O2 signal in a window.If the open eye condition is detected, the analysis decides the direction of eyeball movements. (b) This network has 256 input neurons consists of signals from C3 and C4 channel, one hidden layer with eight neurons and five output neurons representing five eyeball movements.

The number of nodes in the input and output layers of the MLP are dictated by the number of input features and output classes respectively. We utilize a single hidden layer with eight nodes and this ad hoc decision is made prior to the testing session. First, the input layer consists of 128 neurons from O2 signal in a window. The

hidden layer contains eight neurons and connects to two neurons in output layer that represents open and closed eye condition. If open eye condition is detected, the analysis decides the direction of eyeball movements. The input layer consists of 256 neurons for the input data from C3 and C4 signals. They are connected to eight neurons in the hidden layer. In turn, the eight neurons are connected to five neurons in output layer. Finally, the MLP classifies the inputs into five classes of eyeball movements. Signals from the recording session areutilized to train the network using backpropagation algorithm with learning rate at 0.2 and 5000 iterations.

4.0 EXPERIMENTAL RESULTS & DISCUSSION

In this study, the evaluation metrics of accuracy, sensitivity and specificity are determined from the true positive (TP), true negative (TN), false positive (FP) and false negative (FN) to assess the performance of classification techniques.A true positive (TP) is defined as an expected eyelid position or eyeball movement is correctly detected during the experiment. If no detection occurred, the classification output is considered as a false negative (FN) or mistakenly detects as open in eyelid position or no movement in eyeball movement. This is because during open eye (channel O2) and no movement (channel C3 and C4), there are no significant changes can be observed in the respective signals. Therefore, if this condition is expected, the classification output is considered as a true negative. However, if the window interval is detected as other from the aforementioned condition, the output is labeled as false positive (FP) or incorrectly classified.The accuracy represents the percentage of correct decisions while sensitivity and specificity represent the ability toidentify correctly and exclude the condition respectively. These evaluation metrics are computed as follows:

$$Accuracy = \frac{TP + TN}{TP + TN + FP + FN} \tag{8}$$

$$Sensitivity = \frac{TP}{TP + FN} \tag{9}$$

$$Specificity = \frac{TN}{TN + FP} \tag{10}$$

4.1 Thresholding using variance and CTM features

The efficiency of thresholding and classifiers are evaluated in real-time based on a single test. When a participant performing a task, a window of 128 samples is fed to these techniques simultaneously and their performancesare recorded.In total, the participants perform 400 trials for horizontal eyeball movement and 200 trials for eyelid position. The outcomes of the testing session using thresholding and classifiersare outlined inTable 1 and Table 2 respectively.

Variance feature records the highest overall accuracy of 96% with computational time of 0.52s in classification using thresholding. The thresholding of *variance_closed*is utilized to separate the variance into two classes, open and closed eyes in channel O2. In C3 and C4, two thresholds are utilized for each channel to separate the variance into three classes, no movement, center-to-left or right and return-to-center. These thresholds value are utilized for one user is different from another. For example, the *variance_closed* for one of the participant is set at 189 represented by a straight line as shown in Fig.11(a).

Table 1: Performance of the thresholding using variance and CTM features for eyelid position and eyeball movement classification during testing session.

Task	Variance			CTM		
	Accuracy	**Sensitivity**	**Specificity**	**Accuracy**	**Sensitivity**	**Specificity**
Eyelid Position						
Open	0.97	0.95	0.98	0.92	0.91	0.92
Closed	0.98	0.96	0.99	0.95	0.94	0.95
Eyeball Movement						
Center-to-Left	0.97	0.96	0.97	0.91	0.91	0.92
Center-to-Right	0.96	0.95	0.98	0.91	0.91	0.92
Left-to-Center	0.94	0.93	0.96	0.88	0.6	0.89
Right-to-Center	0.93	0.93	0.95	0.87	0.86	0.9
No Movement	0.98	0.97	0.98	0.85	0.83	0.87
Mean	**0.96**	**0.95**	**0.97**	**0.90**	**0.85**	**0.91**
Computational Time		**0.52s**			**0.83s**	

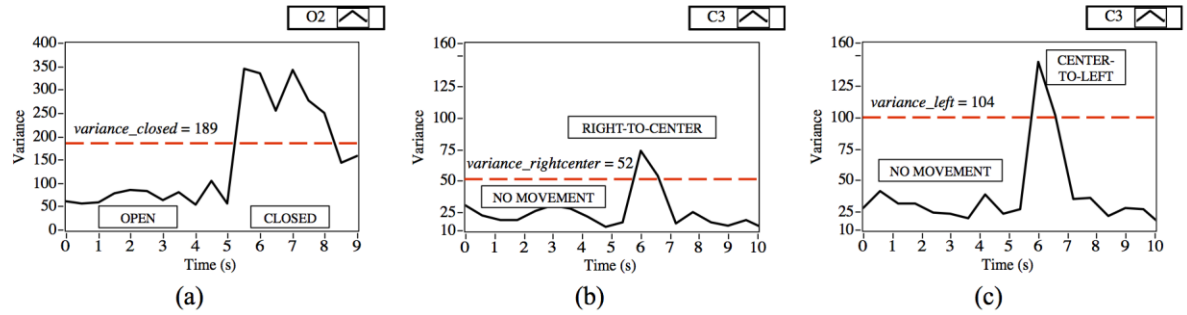

Fig.11: Thresholds set for one of the participant during the testing session. (a) Variance during open and closed eye. The *variance_closed*is represented by a straight line at y = 189 parallel to x-axis. (b), (c)The *variance_rightcenter*and *variance_left* are utilized in C3 to separate the variance into three classes, no movement, right-to-center and center-to-left.

In measuring CTM for eyelid position and eyeball movement classification, x[n+1]-x[n] is plotted against x[n+2]-x[n+1] as depicted in Fig.12. CTM quantifies the degree of variability in second-order difference plot from the ratio of the number of points that fall within a circle with radius (r) over the total numbers of points (n). This variation ismeasured within an optimum radius, r that determines once CTM reaches a value of 0.90.The optimum radius chosen is 0.90 as suggested in [40] to avoid spurious high frequency noisy components at larger radius value.

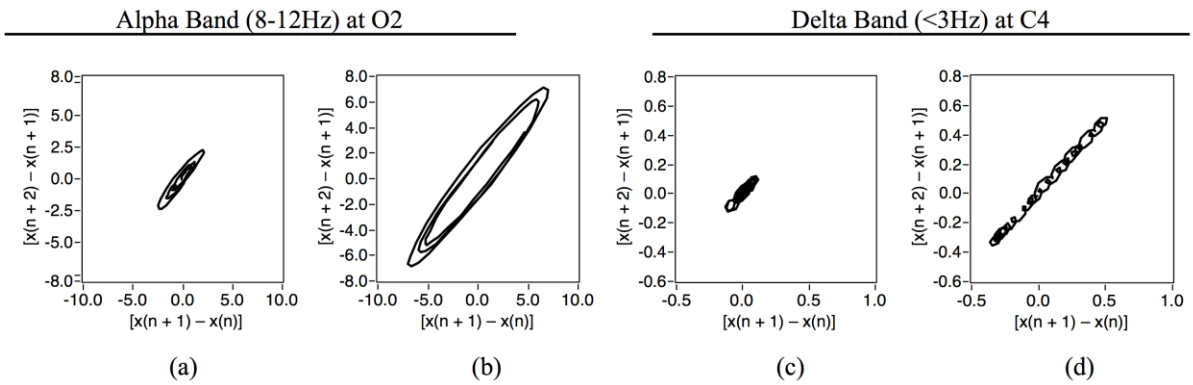

Fig.12: Second-order difference plot in a window of 128 samples during (a) open eye, (b) closed eye,(c) no movement and (d) center-to-right.

A narrow distribution is observed for open eye and a wider distribution for closed eye. In Fig. 13(a), result shows in smaller radius for open eye and larger radius for closed eye to reach CTM value of 0.90. CTM has denoted to low overall accuracy of 90% with computational time 0.83s. The analysis of CTM utilized the time series signals in alpha and delta band to calculate the radius of its variation without amplification. For example, in the case when oscillatory of alpha band islow in amplitude during closed eye, a small differences between the mean r(0.90, open) and r(0.90, closed) makes it hard to differentiate between the two classes.

4.2 Classifiers using MLP and SVM

MLP utilizes supervised learning (i.e.,backpropagation) to create a model from the data during training. The data must be assigned to the respective group at the beginning of the analysis. Then, the MLP assigns the new data to number of groups based on a predetermined model. Table 2 shows that MLP has an average accuracy of 96% and it requires approximately 0.92s for classification.In opposite, SVMs score an average accuracy of 0.98% successive rate during the testing session with approximately 0.53s.In the case of misclassification, class right-to-center is identified as center-to-left and left-to-center is identified as center-to-right. This is also true for misclassification of center-to-right identified as left-to-center and vice versa.

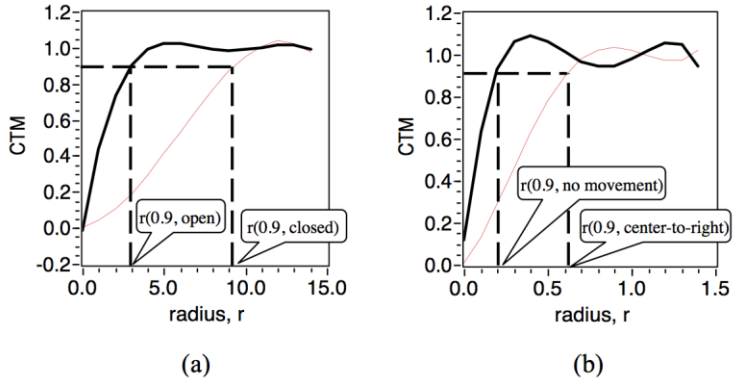

Fig.13:The optimum radius during eyelid position at (a)r(0.90, open) = 2.97, r(0.90, closed) = 9.12,and eyeball movement at (b) r(0.90, no movement) = 0.2, r(0.90, center-to-right) = 0.62are determined when the CTM value reaches 0.90.

The eyeball movement from center to right produces the same positive pulse in C4 and negative pulse in C3, i.e., gaze movement from left to center but vary in strength. However, when subjects are fatigue, the pulse

strength decreases when center-to-right movement is executed, at the same time, the weak pulse represents left-to-center eye gaze.Therefore, the classifiers mistakenly classify the center-to-right as left-to-center. Overall, SVMs produces the highest accuracy rate compare to other thresholding and classifier techniques.

Generally, the factor that contributes to the error is mainly due to the speed of eyeball movement. Low speed of eyeball movementgenerates weak pulses in C3 and C4 andit is difficult to be detected. These errors are caused by fatigue, lack of focus and familiarity, disturbance and confusion.In eyelid position analysis, the errors occur when the ERP of alpha band increases in amplitude due to relaxation and fatigue[43].

Table 2: Performance of the classifiers using MLP and SVM for eyelid position and eyeball movement classification during testing session.

Task	**MLP**			**SVM**		
	Accuracy	**Sensitivity**	**Specificity**	**Accuracy**	**Sensitivity**	**Specificity**
Eyelid Position						
Open	0.96	0.94	0.97	0.99	0.98	1
Closed	0.97	0.95	0.97	0.98	0.97	0.98
Eyeball Movement						
Center-to-Left	0.94	0.93	0.95	0.97	0.97	0.97
Center-to-Right	0.95	0.93	0.96	0.97	0.96	0.97
Left-to-Center	0.95	0.94	0.96	0.99	0.99	0.98
Right-to-Center	0.95	0.94	0.95	0.98	0.98	0.98
No Movement	0.97	0.96	0.98	1	1	1
Mean	**0.96**	**0.94**	**0.96**	**0.98**	**0.98**	**0.98**
Computational Time		**0.92s**			**0.53s**	

5.0 CONCLUSIONS

In this study, EEG and EOG signals are utilizedfor the eyelid positioning and eyeball movements respectively in real-time experiments. The eyelid position is determined by the alpha signal in O2 while the gaze direction is inferred from delta signals in C3 and C4, which contains traces of horizontal eyeball movement. A sliding window is utilizedto capture important cues in the EEG signals for effective classification. Variance and CTM features are extracted from EEG data in the window and utilizedto determine the eyelid position and eyeball movement byusing thresholding. These data are utilized directly as inputs to MLP or SVM classifiers. The performance of both thresholding and classifications are computed and evaluated in real-time based on thetotal 600 signals of eyelid position and eyeball movement. Variance feature scores highest overall accuracy of 96% with computational time of 0.52s for classification using thresholding, while SVM scores0.98% successive rate with computational time of 0.53sfor classification using classifier. Overall, SVM records the highest accuracy rate compare to other features by using thresholding and classifier techniques. From the classification result, the movementdirection of the eyes can be implied and utilizedto control a BCI system. The system has the potential to be utilizedin a practical applicationsuch as cursor positioning and wheelchair navigation.

6.0 ACKNOWLEDGEMENTS

This work was financed by an UMRGgrant (**RP004A-13HNE**) from University of Malaya.

7.0 REFERENCES

[1] Q. X. Nguyen and S. Jo, "Electric Wheelchair Control using Head Pose Free Eye-Gaze Tracker," *Electronics Letters*, Vol. 48, No. 13, Jun 21 2012, pp. 750-752.

[2] H. O. Latif, N. Sherkat, and A. Lotfi, "Telegaze: Teleoperation Through Eye Gaze," *7th IEEE International Conference on Cybernetic Intelligent Systems (CIS 2008),* 2008, pp. 1-6.

[3] T. O. Zander, M. Gaertner, C. Kothe, and R. Vilimek, "Combining Eye Gaze Input with a Brain–Computer Interface for Touchless Human–Computer Interaction," *International Journal of Human-Computer Interaction,* Vol. 27, No. 1, 2010/12/30 2010, pp. 38-51.

[4] C. G. P. Jr, E. L. Naves, P. Pino, E. Losson, A. O. Andrade, and G. Bourhis, "Alternative communication systems for people with severe motor disabilities: a survey," 2011,

[5] Arene, M. D. N. Arene, Hidler, and P. J. Hidler, "Understanding Motor Impairment in the Paretic Lower Limb After a Stroke: A Review of the Literature," *Topics in Stroke Rehabilitation,* Vol. 16, No. 5, 01/01/ 2009, pp. 346-356.

[6] S. Sanei and J. A. Chambers, "Introduction to EEG," in *EEG Signal Processing*, 1st ed West Sussex, England: Wiley, 2007, pp. 1-31.

[7] G. Townsend, B. K. LaPallo, C. B. Boulay, D. J. Krusienski, G. E. Frye, C. K. Hauser, *et al.*, "A Novel P300-Based Brain-Computer Interface Stimulus Presentation Paradigm: Moving Beyond Rows and Columns," *Clinical Neurophysiology,* Vol. 121, No. 7, Jul 2010, pp. 1109-1120.

[8] E. W. Sellers, T. M. Vaughan, and J. R. Wolpaw, "A Brain-Computer Interface for Long-Term Independent Home Use," *Amyotrophic Lateral Sclerosis,* Vol. 11, No. 5, Oct 2010, pp. 449-455.

[9] T. D'albis, R. Blatt, R. Tedesco, L. Sbattella, and M. Matteucci, "A Predictive Speller Controlled by a Brain-Computer Interface Based on Motor Imagery," *ACM Transactions on Computer-Human Interaction,* Vol. 19, No. 3, Oct 2012,

[10] F. Piccione, F. Giorgi, P. Tonin, K. Priftis, S. Giove, S. Silvoni, *et al.*, "P300-Based Brain Computer Interface: Reliability and Performance in Healthy and Paralysed Participants," *Clinical Neurophysiology,* Vol. 117, No. 3, Mar 2006, pp. 531-537.

[11] U. Hoffmann, J. M. Vesin, T. Ebrahimi, and K. Diserens, "An Efficient P300-Based Brain-Computer Interface for Disabled Subjects," *Journal of Neuroscience Methods,* Vol. 167, No. 1, Jan 15 2008, pp. 115-125.

[12] T. Y. Yu, Y. Q. Li, J. Y. Long, and Z. H. Gu, "Surfing the Internet with a BCI Mouse," *Journal of Neural Engineering,* Vol. 9, No. 3, Jun 2012,

[13] M. Marchetti, F. Piccione, S. Silvoni, and K. Priftis, "Exogenous and Endogenous Orienting of Visuospatial Attention in P300-Guided Brain Computer Interfaces: A Pilot Study on Healthy Participants," *Clinical Neurophysiology,* Vol. 123, No. 4, Apr 2012, pp. 774-779.

[14] D. Lederman and J. Tabrikian, "Classification of Multichannel EEG Patterns using Parallel Hidden Markov Models," *Medical & Biological Engineering & Computing,* Vol. 50, No. 4, Apr 2012, pp. 319-328.

[15] Y. Q. Li, J. Y. Long, T. Y. Yu, Z. L. Yu, C. C. Wang, H. H. Zhang, *et al.*, "An EEG-Based BCI System for 2-D Cursor Control by Combining Mu/Beta Rhythm and P300 Potential," *IEEE Transactions on Biomedical Engineering,* Vol. 57, No. 10, Oct 2010, pp. 2495-2505.

[16] I. Iturrate, J. M. Antelis, A. Kubler, and J. Minguez, "A Noninvasive Brain-Actuated Wheelchair Based on a P300 Neurophysiological Protocol and Automated Navigation," *IEEE Transactions on Robotics,* Vol. 25, No. 3, Jun 2009, pp. 614-627.

[17] Y. Arbel, R. Alqasemi, R. Dubey, and E. Donchin, "Adapting the P300-Brain Computer Interface (BCI) for the Control of a Wheelchair-Mounted Robotic Arm System," *Psychophysiology*, Vol. 44, 2007, pp. S82-S83.

[18] B. Rebsamen, C. T. Guan, H. H. Zhang, C. C. Wang, C. Teo, M. H. Ang, *et al.*, "A Brain Controlled Wheelchair to Navigate in Familiar Environments," *IEEE Transactions on Neural Systems and Rehabilitation Engineering*, Vol. 18, No. 6, Dec 2010, pp. 590-598.

[19] D. D. Huang, K. Qian, D. Y. Fei, W. C. Jia, X. D. Chen, and O. Bai, "Electroencephalography (EEG)-Based Brain-Computer Interface (BCI): A 2-D Virtual Wheelchair Control Based on Event-Related Desynchronization/Synchronization and State Control," *IEEE Transactions on Neural Systems and Rehabilitation Engineering*, Vol. 20, No. 3, May 2012, pp. 379-388.

[20] R. Kus, D. Valbuena, J. Zygierewicz, T. Malechka, A. Graeser, and P. Durka, "Asynchronous BCI Based on Motor Imagery with Automated Calibration and Neurofeedback Training," *IEEE Transactions on Neural Systems and Rehabilitation Engineering*, Vol. 20, No. 6, Nov 2012, pp. 823-835.

[21] B. Z. Allison, C. Brunner, V. Kaiser, G. R. Müller-Putz, C. Neuper, and G. Pfurtscheller, "Toward a Hybrid Brain–Computer Interface based on Imagined Movement and Visual Attention," *Journal of Neural Engineering*, Vol. 7, No. 2, 2010, p. 026007.

[22] G. Pfurtscheller, B. Z. Allison, G. Bauernfeind, C. Brunner, T. Solis Escalante, R. Scherer, *et al.*, "The Hybrid BCI," *Frontiers in Neuroscience*, Vol. 4, 2010-April-21 2010,

[23] C. Brunner, B. Z. Allison, D. J. Krusienski, V. Kaiser, G. R. Müller-Putz, G. Pfurtscheller, *et al.*, "Improved Signal Processing Approaches in an Offline Simulation of a Hybrid Brain–Computer Interface," *Journal of neuroscience methods*, Vol. 188, No. 1, 2010, pp. 165-173.

[24] L. Yuanqing, P. Jiahui, W. Fei, and Y. Zhuliang, "A Hybrid BCI System Combining P300 and SSVEP and Its Application to Wheelchair Control," *IEEE Transactions on Biomedical Engineering*, Vol. 60, No. 11, 2013, pp. 3156-3166.

[25] J. Y. Long, Y. Q. Li, H. T. Wang, T. Y. Yu, J. H. Pan, and F. Li, "A Hybrid Brain Computer Interface to Control the Direction and Speed of a Simulated or Real Wheelchair," *IEEE Transactions on Neural Systems and Rehabilitation Engineering*, Vol. 20, No. 5, Sep 2012, pp. 720-729.

[26] P. Horki, T. Solis-Escalante, C. Neuper, and G. Muller-Putz, "Combined Motor Imagery and SSVEP based BCI Control of a 2 DoF Artificial Upper Limb," *Medical & Biological Engineering & Computing*, Vol. 49, No. 5, May 2011, pp. 567-577.

[27] B. Choi and S. Jo, "A Low-Cost EEG System-Based Hybrid Brain-Computer Interface for Humanoid Robot Navigation and Recognition," *Plos One*, Vol. 8, No. 9, 2013, p. e74583.

[28] G. Pfurtscheller, T. Solis-Escalante, R. Ortner, P. Linortner, and G. R. Muller-Putz, "Self-Paced Operation of an SSVEP-Based Orthosis With and Without an Imagery-Based "Brain Switch:" A Feasibility Study Towards a Hybrid BCI," *IEEE Transactions on Neural Systems and Rehabilitation Engineering*, Vol. 18, No. 4, Aug 2010, pp. 409-414.

[29] A. Nijholt and D. Tan, "Brain-Computer Interfacing for Intelligent Systems," *Intelligent Systems, IEEE*, Vol. 23, No. 3, 2008, pp. 72-79.

[30] S. J. Woo, J. Ahn, M. S. Park, K. M. Lee, D. K. Gwon, J.-M. Hwang, *et al.*, "Ocular Findings in Cerebral Palsy Patients Undergoing Orthopedic Surgery," *Optometry & Vision Science*, Vol. 88, No. 12, 2011, pp. 1520-1523.

[31] S. Prasad and S. L. Galetta, "Eye Movement Abnormalities in Multiple Sclerosis," *Neurologic Clinics*, Vol. 28, No. 3, 2010, p. 641.

[32] C.-C. Postelnicu, D. Talaba, and M.-I. Toma, "Controlling a Robotic Arm by Brainwaves and Eye Movement," in *Technological Innovation for Sustainability*. vol. 349, L. Camarinha-Matos, Ed., ed: Springer Berlin Heidelberg, 2011, pp. 157-164.

[33] K. Bonkon, N. Yunjun, and C. Seungjin, "A hybrid EOG-P300 BCI with dual monitors," in *Brain-Computer Interface (BCI), 2014 International Winter Workshop on*, 2014, pp. 1-4.

[34] H. Wang, Y. Li, J. Long, T. Yu, and Z. Gu, "An Asynchronous Wheelchair Control by Hybrid EEG–EOG Brain–Computer Interface," *Cognitive Neurodynamics*, 2014/05/24 2014, pp. 1-11.

[35] A. B. Usakli, S. Gurkan, F. Aloise, G. Vecchiato, and F. Babiloni, "A hybrid platform based on EOG and EEG signals to restore communication for patients afflicted with progressive motor neuron diseases," *2009 Annual International Conference of the Ieee Engineering in Medicine and Biology Society, Vols 1-20*, 2009, pp. 543-546.

[36] O. G. Lins, T. W. Picton, P. Berg, and M. Scherg, "Ocular Artifacts in EEG and Event-Related Potentials I: Scalp Topography," *Brain Topography*, Vol. 6, No. 1, 1993, pp. 51-63.

[37] X.-W. Wang, D. Nie, and B.-L. Lu, "EEG-Based Emotion Recognition Using Frequency Domain Features and Support Vector Machines," in *Neural Information Processing*. vol. 7062, B.-L. Lu, L. Zhang, and J. Kwok, Eds., ed: Springer Berlin Heidelberg, 2011, pp. 734-743.

[38] O. Bai, P. Lin, S. Vorbach, J. Li, S. Furlani, and M. Hallett, "Exploration of Computational Methods for Classification of Movement Intention during Human Voluntary Movement from Single Trial EEG," *Clinical Neurophysiology*, Vol. 118, No. 12, 2007, pp. 2637-2655.

[39] D. Hagemann and E. Naumann, "The Effects of Ocular Artifacts on (Lateralized) Broadband Power in the EEG," *Clinical Neurophysiology*, Vol. 112, No. 2, 2001, pp. 215-231.

[40] R. A. Thuraisingham, Y. Tran, P. Boord, and A. Craig, "Analysis of Eyes Open, Eye Closed EEG Signals using Second-Order Difference Plot," *Medical & Biological Engineering & Computing*, Vol. 45, No. 12, Dec 2007, pp. 1243-1249.

[41] K. Nakayama and K. Inagaki, "A Brain Computer Interface based on neural network with efficient pre-processing," *2006 International Symposium on Intelligent Signal Processing and Communications, Vols 1 and 2*, 2006, pp. 616-619.

[42] K. Nazarpour, Y. Wongsawat, S. Sanei, S. Oraintara, and J. A. Chambers, "A Robust Minimum Variance Beamforming Approach for the Removal of the Eye-Blink Artifacts from EEGs," *2007 Annual International Conference of the IEEE Engineering in Medicine and Biology Society, Vols 1-16*, 2007, pp. 6212-6215.

[43] A. Holm, K. Lukander, J. Korpela, M. Sallinen, #252, and K. M. I. ller "Estimating Brain Load from the EEG," *The Scientific World Journal*, Vol. 9, 2009, pp. 639-651.